3D Topological Relations in Double-Holed Complex Bodies for Shoal-Bar System Evolution

Jialu Liu¹, Liang Leng ^{1,*}

¹ College of Geo-Exploration Science and Technology, Jilin University, Changchun 130026, China liujl24@mails.jlu.edu.cn; lengliang@jlu.edu.cn

Keywords: 3D topological relations, Multi-hole complex bodies, Shoal-bar system.

Abstract

The dynamic evolution of shoal-bar systems in fluvial geomorphology remains challenging to fully capture through conventional observation methods. While multi-dimensional dynamic data enables qualitative analysis of riverine morphology, existing approaches lack effective spatiotemporal topological analysis. This study proposes a novel spatiotemporal modelling framework based on the topological invariance principles of three-dimensional perforated complexes. Focusing on the connectivity preservation in river systems under rotational and scaling transformations, we develop a dual-cavity complex topology model to characterize the dynamic transitions between shoals and sandbars. Compared with traditional single-cavity models, the proposed approach incorporates dynamic cavity features that precisely quantify thalweg elevation changes while resolving the spatiotemporal coupling mechanisms of bar morphology migration. Case study results demonstrate that this approach not only preserves spatial correlations among geomorphic elements but also enables evolutionary trend inversion through topological relation analysis. The methodology provides new theoretical foundations for developing digital twin watershed systems, offering enhanced capabilities for simulating complex fluvial processes.

1. Introduction

The development of shoals into sandbars in river channels exemplifies the self-adjusting morphology of fluvial systems. This morphological evolution alters flow pathways and sediment distribution, critically impacting flood-control safety. Excessive sandbar development may impede channel bifurcation flow, elevating levee-breach risks. For navigation, shoal migration induces abrupt variations in navigable channel depth, jeopardizing vessel safety. Conversely, emerging sandbars generate distinctive ecological habitats for fish spawning and avian nesting (Wang et al., 2024). Consequently, investigating the dynamics of shoal-bar systems enhances both flood control, navigation safety and ecological resource utilization.

However, capturing the spatiotemporal evolution of shoal-bar systems through conventional monitoring remains challenging. Real-time acquisition of field bathymetric and topographic data is operationally intensive and often infeasible. While prior studies frequently utilized remote sensing imagery to quantify sandbar area, this method exhibits limited versatility (Shu et al., 2024).

Multidimensional dynamic spatial data models advance understanding through three dimensions: 3D structure, temporal dynamics, and multiscale processes (Chen et al., 2004). These models not only visualize the spatial associations and distinctions between shoals and sandbars but also delineate their multitemporal evolution. Within this framework, topological relations among geographic entities—representing intrinsic connections between spatial objects invariant under geometric deformation—provide critical qualitative descriptors of geometric configurations in geospatial contexts (Liu et al., 2010). Substantial scholarly work has been conducted on topological relations, yielding several foundational models. Based on pointset topology theory, Egenhofer introduced the 4-Intersection Model (Egenhofer et al., 1991), determining spatial relations by examining intersections of interiors and boundaries between two objects – where a value of 1 denotes non-empty intersection and 0 indicates an empty set. This model was subsequently refined

into the 9-Intersection Model by incorporating the concept of object exteriors, significantly enhancing its expressive capability (Egenhofer et al., 1991). This framework catalysed subsequent research, including Chen's Voronoi-based 9-Intersection Model (V9I) (Chen et al., 2001) and Randell's Region Connection Calculus (RCC) model developed (Randell et al., 1992). The RCC model employs mutually exclusive and complete relations to describe all possible topological relations between spatial regions. Cohn later extended this approach to characterize topological relations among fuzzy objects. Building upon the 4IM and 9IM frameworks, Deng Min et al. proposed a 4-Intersection Difference Model using intersections and differences among object interiors, boundaries, and wholes (Deng et al., 2005). These early models primarily addressed topology between simple objects, whereas real-world geographic features often exhibit complexity, such as lakes containing islands, necessitating representations for holed regions. In 1994, Egenhofer formalized topological relations between holed objects A and B through four components: relations between the wholes of A and B, the whole of A and each hole of B, each hole of A and the whole of B, and each hole of A and each hole of B (Egenhofer et al., 1994). Subsequent research expanded this to include relations between holed regions and simple regions (Deng et al., 2008; Li et al., 2012), dual-holed regions and simple regions (Li et al., 2012), and concave regions and holed regions (Li et al., 2013). Ouyang Jihong et al. further developed an extended 9-Intersection Model for holed regions (Ouyang et al., 2009). Shen Jingwei et al. advanced the 25-Intersection Model, decomposing holed polygonal objects into five elements: interior, inner boundary, interior within inner boundary, outer boundary, and exterior beyond outer boundary (Shen et al., 2016). For multi-holed regions, Leng Liang et al. established a generalized 9-Intersection Model where intersection values between multiple holes are represented as binary sequences converted to decimal notation – significantly surpassing prior models in discriminative power (Leng et al., 2022).

While these methods demonstrate progressive refinement for holed regions, their application remains constrained to two-

dimensional contexts. For instance, lakes with central islands can be visualized in 2D, whereas submerged shoals within river channels-which do not breach the water surface-cannot be adequately represented. Moreover, accurately representing the morpho dynamic process from shoal to sandbar fundamentally demands three-dimensional volumetric characterization. This intrinsic limitation conclusively highlights the essential requirement for 3D topological relations—particularly critical when modelling dynamic interactions between discrete volumetric entities. Shen Jingwei et al. addressed this gap using a dimensionally extended 9-Intersection Model, delineating eight meaningful topological relations between volumetric entities: disjoint, touches, overlaps, covers, contains, equal, coveredBy, and within (Shen et al, 2012). Zhang Jun et al. segmented threedimensional holed objects into five subcomponents, revealing a conceptual parallel to the 25-Intersection Model for holed polygons (Zhang et al., 2008). Di Shuang advanced the framework through a 3D 9+-Intersection Model, investigating relations between single-holed complex objects and simple solids, between two single-holed complex objects, and between multiholed complex objects and simple solids (Di, 2015). Although these studies represent progress in volumetric topology, significant limitations persist-specifically the absence of frameworks for modeling relations between two multi-holed complex objects, along with prior analyses being restricted to cotemporal yet distinct entities.

The uniqueness of shoal-bar systems lies in their representation of dynamic variations across temporal states within the same fluvial entity, characterized by three-dimensional complex objects containing multiple voids. Existing frameworks, including the classical 9-Intersection Model and its derivatives, fail to comprehensively characterize such configurations, exhibiting limited discriminative capability. Building upon prior inferences of 3D complex object topology and inspired by 2D multi-holed regional relations, this study proposes a threedimensional double-holed complex body topology model specifically for riverine shoal-bar system. This model abstracts the two river states in different times and spaces into two complex entities with double holes. By exploring the topological relation between them, it can determine the evolution of the shole-bar system in the river, and also verifies the completeness of the model by comparing with other methods.

The main contributions of this research can be summarized as follows: (1) A double-hole complex body model for the dynamic evolution of the shole-bar system in rivers is proposed; (2) A method for determining the topological relation between objects based on the model is introduced, and some typical topological relation scenarios are described; (3) The topological relation inference of the classic scenarios of shole-bar using the above two points is realized.

2. Methodology

Implementing the double-holed complex body model to diagnose shoal-bar system dynamics involves two critical phases: Construct geometric topological models of real-world problems and determine the topological relation between complex bodies at two different moments.

2.1 Construct a geometric topological model

In order to abstract the river and its internal shoals and sandbars into a geometric model that is conducive to the determination of topological relations, the following principles need to be followed: (1) The characteristics and properties of the shole-bar

system should remain unchanged, so that the model has strong representativeness; (2) The representation form should be simple and intuitive, facilitating understanding.

Based on these principles, in this study, the river is represented by a cube with holes, and the shoals and sandbars are represented by elliptical cylinders within the cube. To facilitate the extension to the case of several holes, this study defines a cube with holes containing two holes, that is, two elliptical cylinders, and regards these two elliptical cylinders as shoals or sandbars separated by a certain distance, even if the sediment continuously accumulates causing the shoals and sandbars to continuously develop, they will not come into contact. Therefore, the two elliptical cylinders do not intersect. Considering the real situation, the sholes are formed by the suspended load (sand, gravel, etc.) of the riverbed continuously accumulating underwater, and their surface elevation is always lower than the normal water level of the river. Even in the dry season, there is no exposure manifestation. The sandbars are the patchy accumulations that protrude above the water surface when the volume of the sediment exceeds the accommodation threshold of the river channel. They maintain a stable surface exposure state during the flood season. Therefore, the bottoms of the shoals and sandbars are all connected to the riverbed, but they will not touch the riverbank. The shoals do not touch the water surface, while the sandbars will contact the water surface. Thus, the bottom of the cube representing the river indicates the riverbed, the top indicates the water surface, the side surfaces indicate the riverbanks on both sides and the distant rivers that do not contact the shole-bar system, and the interior of the cube indicates the flowing water. The top surface of the elliptical cylinder representing the sandbar indicates the part in contact with the water surface, but to facilitate the determination of topological relations, the part of the sandbar exceeding the water surface will not be represented. As long as the top surface coincides with the top surface of the cube, it indicates that this must be the sandbar. And the elliptical cylinder with a top surface not coinciding with the top surface of the cube must represent the shoals below the water surface. Whether it is the shoals or the sandbars, the bottom of the elliptical cylinder is always in contact with the bottom of the cube, and the side surfaces do not contact the side surfaces of the cube.

Furthermore, the topological relation between the cube and the two elliptical-cylindrical cavities is defined as Covers, the outer boundaries are connected, and the intersection of the elliptical cylinder and the cube is the entire elliptical cylinder.

The state of the shoal-bar system is divided into two moments, t1 and t2. By analysing the topological relation of two complex bodies with double holes, the dynamic changes of the shoalsandbar system can be determined. The two complex bodies are named A and B, representing the initial and final states of the river and shoal-sandbar system. The elliptical cylinders inside are called "holes", and since the two different holes within the same cube have unique meanings, hole1 and hole2 are used to distinguish them. Based on the 9-Intersection Model and 25-Intersection Model, this study expands and defines the elements of the complex bodies. Taking cube A as an example, the first hole is A_1^h , the second hole is A_2^h , the boundary of the first hole is ∂A_1^h , the boundary of the second hole is ∂A_2^h , the interior of cube A is A^0 , the outer boundary of A is $\partial_{out}A$, and the exterior of A is A^- . When representing the content of the hole or the content of the cube, the set is an open set, such as A_1^h , A_2^h , A_2^0 ; when representing the boundary of the hole or the outer boundary of the cube, the set is a closed set, such as ∂A_1^h , $\partial_{out} A$; when representing the region of the external topological space, the set is also an open set, such as A^- .

$$R_{DH}(A,B) = \begin{bmatrix} A_{1}^{h} \cap B_{1}^{h} & A_{1}^{h} \cap B_{2}^{h} & A_{1}^{h} \cap \partial B_{1}^{h} & A_{1}^{h} \cap \partial B_{2}^{h} & A_{1}^{h} \cap \partial B_{2}^{h} & A_{1}^{h} \cap B^{0} & A_{1}^{h} \cap \partial_{\text{out}} B & A_{1}^{h} \cap B^{-} \\ A_{2}^{h} \cap B_{1}^{h} & A_{2}^{h} \cap B_{2}^{h} & A_{2}^{h} \cap \partial B_{1}^{h} & A_{2}^{h} \cap \partial B_{2}^{h} & A_{2}^{h} \cap B^{0} & A_{2}^{h} \cap B^{0} & A_{2}^{h} \cap \partial_{\text{out}} B & A_{2}^{h} \cap B^{-} \\ \partial A_{1}^{h} \cap B_{1}^{h} & \partial A_{1}^{h} \cap B_{2}^{h} & \partial A_{1}^{h} \cap \partial B_{1}^{h} & \partial A_{1}^{h} \cap \partial B_{2}^{h} & \partial A_{1}^{h} \cap B^{0} & \partial A_{1}^{h} \cap \partial_{\text{out}} B & \partial A_{1}^{h} \cap B^{-} \\ \partial A_{2}^{h} \cap B_{1}^{h} & \partial A_{2}^{h} \cap B_{2}^{h} & \partial A_{2}^{h} \cap \partial B_{1}^{h} & \partial A_{2}^{h} \cap \partial B_{2}^{h} & \partial A_{2}^{h} \cap B^{0} & \partial A_{2}^{h} \cap \partial_{\text{out}} B & \partial A_{1}^{h} \cap B^{-} \\ A^{0} \cap B_{1}^{h} & A^{0} \cap B_{2}^{h} & A^{0} \cap \partial B_{1}^{h} & A^{0} \cap \partial B_{2}^{h} & A^{0} \cap B^{0} & A^{0} \cap \partial_{\text{out}} B & A^{0} \cap B^{-} \\ \partial_{\text{out}} A \cap B_{1}^{h} & \partial_{\text{out}} A \cap B_{2}^{h} & \partial_{\text{out}} A \cap \partial B_{1}^{h} & \partial_{\text{out}} A \cap B_{2}^{h} & \partial_{\text{out}} A \cap B^{0} & A^{-} \cap \partial_{\text{out}} B & \partial_{\text{out}} A \cap B^{-} \\ A^{-} \cap B_{1}^{h} & A^{-} \cap B_{2}^{h} & A^{-} \cap \partial B_{1}^{h} & A^{-} \cap \partial B_{2}^{h} & A^{-} \cap B^{0} & A^{-} \cap B_{\text{out}} B & A^{-} \cap B^{-} \end{bmatrix}$$

The double-holed complex body model defined in this context can formally be abbreviated as the DH Model. Topological relations between complex bodies A and B are determined by evaluating intersections across their seven constituent elements. This process yields a 7×7 matrix representing two double-holed complex body topology, formalized in Equation (1), where each matrix element encodes binary intersection states: 0 denotes empty intersection, while 1 indicates non-empty overlap.

2.2 Topological relations of complex bodies

Given the intricate nature of topological relations between double-holed complex bodies, we adopt a hierarchical approach: First, simplify bodies A and B as solid volumes without holes, considering only their interior, boundary, and exterior components. This allows preliminary classification using the eight fundamental topological relations for simple bodies: Disjoint, Touches, Overlaps, Covers, Contains, Equal, CoveredBy, and Within. We then refine this classification by incorporating interactions between their holes. For systematic analysis, the cylindrical holes in initial-state body A are designated h_1 and h_2 , while terminal-state body B's holes are labeled h_1' and h_2' – all modelled as closed sets.

When the topological relation between A and B is Disjoint, the two holes h_1 and h_2 of A and the two holes h'_1 and h'_2 of B must be in a Disjoint relation. As shown in Figure 1.

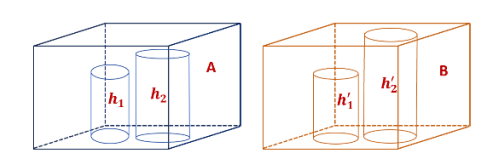


Figure 1. Disjoint topological relation between A and B.

Its matrix can be expressed as Equation (2).

$$R(A,B) = \begin{bmatrix} 0 & 0 & 0 & 0 & 0 & 0 & 1\\ 0 & 0 & 0 & 0 & 0 & 0 & 1\\ 0 & 0 & 0 & 0 & 0 & 0 & 1\\ 0 & 0 & 0 & 0 & 0 & 0 & 1\\ 0 & 0 & 0 & 0 & 0 & 0 & 1\\ 1 & 1 & 1 & 1 & 1 & 1 & 1 \end{bmatrix}$$
 (2)

When the topological relation between A and B is Touches, there are two cases of contact. The first is that the side surfaces of A and B are in contact. At this time, the two holes h_1 , h_2 of A and the two holes h_1' , h_2' of B must be in a Disjoint relation. The second is that the top and bottom surfaces of A and B are in contact. It is possible that A is above B or B is above A. Whether the two holes h_1 , h_2 of A and the two holes h_1' , h_2' of B are in a Touches relation depends on whether the elliptical cylinders within the complex body below touch the top surface. If none of the elliptical cylinders within the complex body below touch the top surface, which represents that they are all shoals rather than

sandbars, then the holes of the upper cube and the holes of the lower cube must not be in touch; if there is an elliptical cylinder touching the top surface, then h_1 , h_2 and h_1' , h_2' may be in touch, and the specific situation can be detailedly counted according to the mathematical permutation and combination method.

This article selects a typical case to illustrate. As shown in Figure 2, the bottom surface of A is connected to the top surface of B, while h_1 and h_2 Disjoint from h_1' but all touch h_2' .

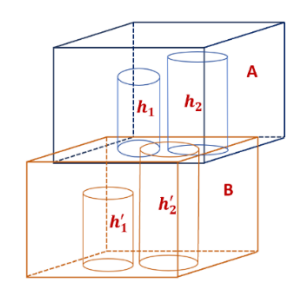


Figure 2. An example of Touches topological relation between A and B.

Its matrix can be expressed as Equation (3).

$$R(A,B) = \begin{bmatrix} 0 & 0 & 0 & 0 & 0 & 0 & 1 \\ 0 & 0 & 0 & 0 & 0 & 0 & 1 \\ 0 & 0 & 0 & 1 & 0 & 1 & 1 \\ 0 & 0 & 0 & 1 & 0 & 1 & 1 \\ 0 & 0 & 0 & 0 & 0 & 0 & 1 \\ 0 & 0 & 0 & 1 & 0 & 1 & 1 \\ 1 & 1 & 1 & 1 & 1 & 1 & 1 \end{bmatrix}$$
(3)

When the topological relation between complex bodies A and B is Overlaps, it indicates that their interiors intersect but the intersection area differs from either spatial object individually. Numerous topological scenarios become possible between these complex bodies. Broadly two classifications exist: First, while A and B intersect, their constituent holes $(h_1, h_2 \text{ in A and } h'_1, h'_2)$ in B) maintain mutually Disjoint relations, allowing diverse relations to form between bodies and cross-body holes - for instance, A might relate to h'_1 and h'_2 through Disjoint, Touches, Overlaps, Covers, or Contains relations. Second, at least one hole pair establishes non-Disjoint relations, meaning not only do the bodies intersect, but their holes physically interact through potential connections like Disjoint, Touches, Overlaps, Covers, Contains, Equal, CoveredBy or Within. This significantly increases complexity - we might observe h_1 Touching h_1' while Overlapping h_2' , concurrently with h_2 being CoveredBy h_1' but remaining Disjoint from h_2' . Countless permutations emerge though not all can be enumerated. Crucially, since holes within the same cube must remain Disjoint, these interactions become constrained rather than arbitrary. Specifically, the relation of h_1 with h'_1 directly limits its possible relations with h_2' as summarized in Table 1, when h_1 and h'_1 are Disjoint, its connection with h'_2 becomes

175

unrestricted and may adopt any of the eight fundamental bodyto-body topological relations.

h_1 with h'_1	h_1 with h'_2		
Touches	Disjoint, Touches, Overlaps, Covers, Contains		
Overlaps	Disjoint, Touches, Overlaps, Covers, Contains		
Covers	Disjoint, Touches, Overlaps, Covers, Contains		
Contains	Disjoint, Touches, Overlaps, Covers, Contains		
Equal, CoveredBy, Within	Disjoint		

Table 1. Topological relation correspondence between h_1 vs. h'_1 and h_1 vs. h'_2 .

It can be proved by contradiction that when the relation between h_1 and h_1' is Touches, Overlaps, Covers and Contains, then h_1 and h_1' must be in contact. If the relation between h_1 and h_2' is equal, Then h_2' is also in contact with h_1' , which violates the property that two holes cannot intersect in our definition; If the relation between h_1 and h_2' is coveredby or within, then h_1 must be in the interior of h_2' , which also violates the property that h_1' and h_2' must be separated from each other. However, when the relation between h_1 and h_1' is Equal, CoveredBy, Within, h_1 is either equal to h_1' or within h_1' , it can only be separated from h_2' . Similarly, the relation between h_1 and h_1' and h_2' will also affect the relation between h_2 and h_1' and h_2' . Table 2 shows the corresponding relation between h_2 and h_1' when h_1 is related to h_1' . When h_1' becomes h_2' , it is the same as in Table 2.

h_1 with h_1^\prime	h_2 with h_1'	
Touches	Disjoint, Touches, Overlaps, CoveredBy, Within	
Overlaps	Disjoint, Touches, Overlaps, CoveredBy, Within	
Covers, Contains, Equal	Disjoint	
CoveredBy	Disjoint, Touches, Overlaps, CoveredBy, Within	
Within	Disjoint, Touches, Overlaps, CoveredBy, Within	

Table 2. Topological relation correspondence between h_1 vs. h'_1 and h_2 vs. h'_1 .

Based on the above correspondence, there are too many cases of complex A and B overlapping, so this article selects a typical case to illustrate. As shown in Figure 3, h_1 maintains a Touches connection with h_1' while remaining Disjoint from h_2' . Concurrently, h_2 establishes Overlaps relations with both h_1'

and h'_2 and the outer boundary of B intersects h_1 , and the outer boundary of A is tangent to h'_2 .

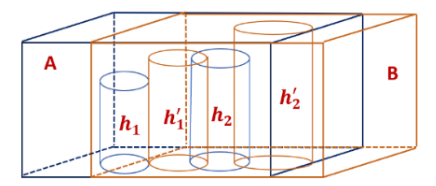


Figure 3. An example of Overlaps topological relation between A and B.

Its matrix can be expressed as Equation (4).

$$R(A,B) = \begin{bmatrix} 0 & 0 & 0 & 0 & 1 & 1 & 1 \\ 1 & 1 & 1 & 1 & 1 & 0 & 0 \\ 0 & 0 & 1 & 0 & 1 & 1 & 1 \\ 1 & 1 & 1 & 1 & 1 & 1 & 0 \\ 1 & 1 & 1 & 1 & 1 & 1 & 1 \\ 0 & 0 & 1 & 1 & 1 & 1 & 1 \\ 0 & 0 & 0 & 0 & 1 & 1 & 1 \end{bmatrix}$$
(4)

When the topological relation between complex bodies A and B is defined as Covers, it signifies that the interior of spatial object A contains the interior of spatial object B, while their boundaries intersect, and A is not equivalent to B. This configuration positions B within A's interior, where B exhibits smaller volumetric extent than A. Under these conditions, the topological relations between h_1 , h_2 and h'_1, h'_2 may manifest in diverse configurations, potentially encompassing any of the eight fundamental topological relations, though constrained by the limitations previously documented in Tables 1 and 2. To concretely illustrate this complexity, Figure 4 depicts a representative scenario where B is positioned within A with its upper and rear surfaces contacting A's external boundary, while simultaneously h_1 maintains Overlaps relations with both h'_1 and h'_2 , and h_2 remains Disjoint from h'_1 yet exhibits an Overlaps interaction with h'_2 .

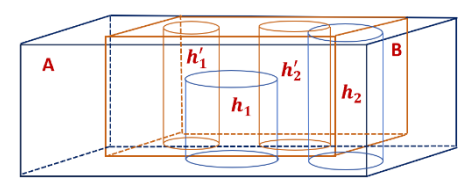


Figure 4. An example of Covers topological relation between A and B.

Its matrix can be expressed as Equation (5).

When the topological relation between complex bodies A and B is Contains, it signifies that A completely encloses B without boundary intersection, differing from the Covers relation solely in the absence of boundary contact. To demonstrate this configuration, Figure 5 illustrates a representative case where B resides entirely within A's interior with no boundary contact between the two bodies. And h_1 maintains an Overlaps relation

with h'_1 while remaining Disjoint from h'_2 , h_2 establishes a Touches connection with h'_1 and a Contains relation with h'_2 .

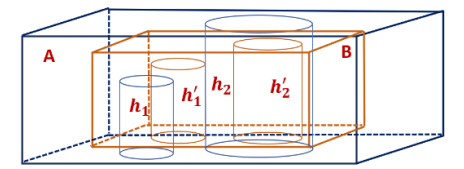


Figure 5. An example of Contains topological relation between A and B.

Its matrix can be expressed as Equation (6).

When the topological relation between A and B is Equal, the topological relations of h_1 , h_2 and h'_1 , h'_2 remain diverse. One of the most special cases is that h_1 and h'_1 are equal, and h_2 and h'_2 are also equal. Only then are the two complex bodies truly equal. This study illustrates a representative scenario as Figure 6, h_1 Overlaps h'_1 but is Disjoint from h'_2 , while h_2 remains Disjoint from h'_1 and is CoveredBy h'_2 .

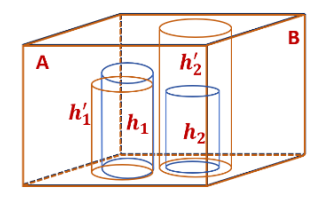


Figure 6. An example of Equal topological relation between A and B.

Its matrix can be expressed as Equation (7).

$$R(A,B) = \begin{bmatrix} 1 & 0 & 1 & 0 & 1 & 0 & 0 \\ 0 & 1 & 0 & 0 & 0 & 0 & 0 \\ 1 & 0 & 1 & 0 & 1 & 1 & 0 \\ 0 & 1 & 0 & 1 & 0 & 1 & 0 \\ 1 & 1 & 1 & 1 & 1 & 0 & 0 \\ 0 & 0 & 1 & 1 & 0 & 1 & 0 \\ 0 & 0 & 0 & 0 & 0 & 0 & 1 \end{bmatrix}$$
(7)

When considering the topological relations CoveredBy and Within between complex bodies A and B, these configurations fundamentally mirror the spatial interactions observed in Covers and Contains relations respectively. The core distinction lies solely in reversing the volumetric hierarchy — specifically, designating which entity functions as the volumetrically dominant enclosing body. Consequently, We omit detailed explanation of CoveredBy/Within cases since their logic mirrors the established Covers/Contains principles.

3. Experiment and Discussion

As described earlier, the double-holed complex body model employs matrices to represent topological relationships between two objects each containing two holes. To validate model completeness, comparative experiments with prior approaches are essential to reveal their respective strengths and weaknesses. The 9-intersection and 25-intersection models remain the most prevalent classical frameworks, with matrix expressions formalized in Equations (8) and (9) respectively. Although later studies proposed 3D topological relations for perforated bodies, such models remain fundamentally restricted to single-hole cases and thus essentially constitute 25-intersection variants; they merely redefine the exterior beyond inner boundaries as hole interiors – a distinction solely reflecting whether holes are treated as independent entities – while matrix values remain unchanged. Consequently, these derivative models are not separately presented.

$$R_{9\mathrm{IM}}(A,B) = \begin{bmatrix} A^0 \cap B^0 & A^0 \cap \partial B & A^0 \cap B^- \\ \partial A \cap B^0 & \partial A \cap \partial B & \partial A \cap B^- \\ A^- \cap B^0 & A^- \cap \partial B & A^- \cap B^- \end{bmatrix}$$
(8)

$$R_{\mathrm{25IM}}(A,B) = \begin{bmatrix} A^0 \cap B^0 & A^0 \cap \partial B_E & A^0 \cap \partial B_1 & A^0 \cap \partial B_E^- & A^0 \cap \partial B_I^- \\ \partial A_E \cap B^0 & \partial A_E \cap \partial B_E & \partial A_E \cap \partial B_1 & \partial A_E \cap \partial B_E^- & \partial A_E \cap \partial B_I^- \\ \partial A_1 \cap B^0 & \partial A_1 \cap \partial B_E & \partial A_1 \cap \partial B_1 & \partial A_1 \cap \partial B_E^- & \partial A_1 \cap \partial B_I^- \\ A_E^- \cap B^0 & A_E^- \cap \partial B_E & A_E^- \cap \partial B_1 & A_E^- \cap \partial B_E^- & A_E^- \cap \partial B_I^- \\ A_1^- \cap B^0 & A_1^- \cap \partial B_E & A_1^- \cap \partial B_1 & A_1^- \cap \partial B_E^- & A_1^- \cap \partial B_I^- \end{bmatrix}$$

To benchmark against established methods, this study selects a classic shoal-bar scenario demonstrating the matrix's discriminative power; it examines two distinct fluvial cases (Figure 7) where initial dual shoals evolve differently: Scenario A shows vertical aggradation and displacement of both shoals driven by riverbed uplift and positional migration, while Scenario B features shoal accretion and shifting under stable riverbed elevation with lateral channel shift, caused by bank widening, water-level rise and overall channel movement compared to the baseline.

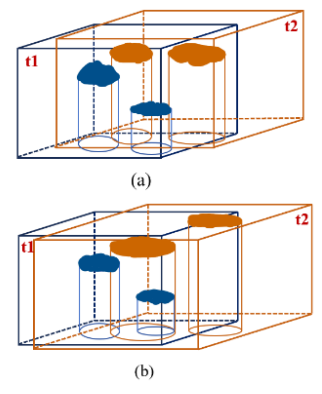


Figure 7. Example Illustration of Shoal-Bar System Dynamic Evolution.

This scientific scenario transforms into a topological model visualized in Figure 8, where example (a) demonstrates: h_1' Overlaps h_1 while Touches h_2 , h_2' remains Disjoint from h_1 yet Overlaps h_2 , with both h_1 and h_2 penetrating the surface of body B, and both h_1' and h_2' penetrating the surface of body A; conversely, example (b) exhibits: h_1' Overlaps h_1 while Covers h_2 , h_2' maintains Disjoint status from h_1 and h_2 , as h_1 penetrates B's surface while h_2' penetrates A's surface, collectively manifesting differential hole-boundary interactions across evolving fluvial states.

Evidently, both 9-intersection and 25-intersection models fail to explicitly define individual holes within holed bodies, fundamentally preventing discrimination between configurations (a) and (b). Specifically, the 9-intersection model conflates all boundaries—including external boundaries and hole boundaries—into a single boundary element, while the 25-intersection model aggregates hole boundaries and interiors

under generalized interior/exterior classifications, obscuring critical distinctions.

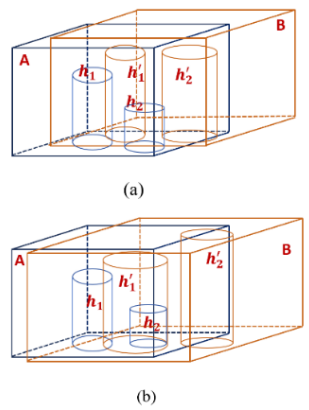


Figure 8. Schematic diagram of the double-holed complex body model for shoal-bar system dynamics.

In contrast, the proposed DH Model comprehensively encodes each topological element, overcoming limitations in representing nuanced intersection values. Applying these three matrix representations to examples (a) and (b) in Figure 8 yields comparative results (Table 3), clearly demonstrating that despite substantial topological differences, both classical models employ identical matrices whereas only the DH Model generates distinct matrices to differentiate the scenarios.

The proposed matrix distinguishes these scenarios through differential element values; for example, when the interior of h_2 intersects that of h_1' while their boundaries also intersect, and h_2 does not intersect the interior of body B, this configuration represents h_2 being covered by h_1' . This model not only exhibits strong discriminative capacity for diverse topological relationships between complex bodies but also enables precise determination of any entity's topological status through specific element values, combining geometric-computational advantages to concisely address scientific problems.

Objects	9-Intersection Model	25-Intersection Model	DH Model
Topological relations in Figure 8(a)	$\begin{bmatrix} 1 & 1 & 1 \\ 1 & 1 & 1 \\ 1 & 1 & 1 \end{bmatrix}$	$\begin{bmatrix} 1 & 1 & 1 & 1 & 1 \\ 1 & 1 & 1 & 1 & 1 \\ 1 & 1 &$	$\begin{bmatrix} 1 & 0 & 1 & 0 & 1 & 1 & 1 \\ 0 & 1 & 0 & 1 & 1 & 1 & 1 \\ 1 & 0 & 1 & 0 & 1 & 1 & 1 \\ 0 & 1 & 1 & 1 & 1 & 1 & 1 \\ 1 & 1 & 1 & 1$
Topological relations in Figure 8(b)	$\begin{bmatrix} 1 & 1 & 1 \\ 1 & 1 & 1 \\ 1 & 1 & 1 \end{bmatrix}$	$\begin{bmatrix} 1 & 1 & 1 & 1 & 1 \\ 1 & 1 & 1 & 1 & 1 \\ 1 & 1 &$	$\begin{bmatrix} 1 & 0 & 1 & 0 & 1 & 1 & 1 \\ 1 & 0 & 0 & 0 & 0 & 0 & 0 \\ 1 & 0 & 1 & 0 & 1 & 1 & 1 \\ 1 & 0 & 1 & 0 & 0 & 0 & 0 \\ 1 & 1 & 1 & 1 & 1 & 1 & 1 \\ 0 & 1 & 0 & 1 & 1 & 1 & 1 \end{bmatrix}$

Table 3. Comparison of two topological relationships using three distinct topological model.

Even with altered matrix values, we can still determine the topological relationship between complex bodies, thereby revealing the initial-to-terminal dynamic evolution of shoal-bar systems. Future extensions to bodies with m and n holes will maintain this discriminative approach, though reducing computational load becomes critical as matrix dimensions increase indefinitely.

Consequently, the comparative analysis demonstrates that the proposed matrix model enforces rigorous constraints; it overcomes limitations of existing models confined to 2D porous regions or 3D single-hole complex bodies, enabling precise discrimination of topological relationships between double-holed (and even multi-holed) complex bodies. Consequently, this capability reveals intricate fluvial processes – including riverbed aggradation/degradation, shoal accretion dynamics, and sandbar migration patterns – throughout temporal evolutionary phases.

4. Conclusion

This research addresses the challenge of capturing dynamic shoal-bar system evolution in fluvial geomorphology through conventional methods by constructing a double-holed complex body model that characterizes system evolution across spatiotemporal states. The methodology abstracts river channels

as perforated cubes and shoal-bar systems as dual ellipticalcylindrical holes within these cubic structures; it defines intersection relations between interior, boundary, and exterior components of complex bodies to establish a 7×7 topological matrix, thereby enabling precise quantification of threedimensional dynamic processes including shoal vertical accretion and channel migration. Compared to traditional 2D multi-hole models and 3D simple-body topological approaches, this model breaks dimensional and cavity-count constraints while preserving the spatial integrity of geomorphic features; its topological matrix enables dynamic process deduction including shoal accretion and sandbar migration. Validation through classic shoal evolution scenarios demonstrates superior discriminative capability against 9-intersection and 25-intersection models when handling complex topological configurations, confirming method completeness. This provides novel theoretical foundations for digital twin watershed development with significant preventive value against channel blockages from excessive sandbar growth and navigational hazards triggered by sudden shoal migration.

Future research can be further developed. Firstly, the current two holes can be expanded to a more general multi-hole scenario. By extending the matrix system, the model can handle complex bodies with any number of holes. Moreover, the number of

complex bodies can be dynamically expanded through iterative processes. By continuously comparing the latest state with a certain historical moment, a dynamic evolution comparison chart can be formed, which can visually display the process of how shoals gradually become sandbars, and how sandbars migrate or are weakened. Secondly, multi-source data fusion can be used to achieve the generalization of the model. Currently, the model has completed geometric abstraction. In the future, it can integrate centimetre-level sandbar elevations obtained by unmanned aerial vehicle laser radar, changes in sandbar boundaries captured by satellite images, and underwater riverbed topography obtained by sonar, to construct a three-dimensional topological entity that conforms to real-world problems. Thus, it can realize the deduction of complex landforms and real-time early warning for dynamic monitoring.

References

- Chen, J., Li, C., Li, Z.L., 2001. A Voronoi-based 9-intersection model for spatial relations. *Int. J. Geogr. Inf. Sci.*, 15(3), 201-220.
- Chen, J., Li, Z.L., Jiang, J., Zhu, Q., 2004. Research on multidimensional dynamic GIS spatial data model and methods. *Geomat. Inf. Sci. Wuhan Univ.*, 29(10), 858-862.
- Deng, M., Liu, W.B., Feng, X.Z., 2005. A formal model for topological relations between areal objects in GIS. *Acta Geod. Cartogr. Sin.*, 34(1), 85-90.
- Deng, M., Li, Z.L., Li, G.Q., 2008. Hierarchical expression of topological relations between simple regions and regions with holes. *Acta Geod. Cartogr. Sin.*, 37(3), 330-337.
- Di, S., 2015. Expression of topological relations for 3D volumes with holes. Shandong Norm. Univ., Jinan, China.
- Egenhofer, M.J., Clementini, E., Di Felice, P., 1994. Topological relations between regions with holes. *Int. J. Geogr. Inf. Syst.*, 8(2), 129-142. doi.org/10.1080/02693799408901990
- Egenhofer, M.J., Franzosa, R.D., 1991. Point-set topological spatial relations. *Int. J. Geogr. Inf. Syst.*, 5(2), 161-174. doi.org/10.1080/02693799108927841
- Egenhofer, M.J., Herring, J.R., 1991. Categorizing binary topological relationships between regions, lines and points in geographic database. Dep. Surv. Eng., Univ. Maine, Orono, ME, USA.
- Leng, L., Wang, F., Wang, M., Yang, G., Niu, X., Zhang, X., 2022. A Generalized 9-Intersection Model for Topological Relations between Regions with Holes. *ISPRS Int. J. Geo-Inf.*, 11(4), 218. doi.org/10.3390/ijgi11040218
- Li, J., Ouyang, J.H., Chen, G., Wang, Z.X., 2013. Representation of topological relations between a concave region and a simple region. *J. Jilin Univ. Eng. Technol. Ed.*, 43(2), 386-390. doi.org/10.13229/j.cnki.jdxbgxb2013.02.016
- Li, J., Ouyang, J.H., Wang, G.W., Chen, G., 2012. Representation of topological relations between a single-hole region and a simple region. *J. Jilin Univ. Sci. Ed.*, 50(6), 1209-1213. doi.org/10.13413/j.cnki.jdxblxb.2012.06.011
- Li, J., Ouyang, J.H., Wang, Z.X., 2012. Topological relations between a double-hole region and a simple region. *J. Jilin Univ.*

- Eng. Technol. Ed., 42(5), 1214-1218. doi.org/10.13229/j.cnki.jdxbgxb2012.05.009
- Liu, X., Liu, W.B., Li, C.M., 2010. Description and Qualitative Reasoning of 3D Spatial Relations. *Surv. Map. Press*, Beijing.
- Ouyang, J.H., Huo, L.L., Liu, D.Y., Fu, Q., 2009. Extended 9-intersection model for topological relations of regions with holes. J. Jilin Univ. Eng. Technol. Ed., 39(6), 1595-1600. doi.org/10.13229/j.cnki.jdxbgxb2009.06.035
- Randell, D., Cui, Z., Cohn, A., 1992. A spatial logic based on regions and connection. *Proc. 3rd Int. Conf. Knowl. Represent. Reason.*, New York, 165-176.
- Shen, J.W., Wen, Y.N., Lu, G.N., Wu, M.G., 2012. Research on 3D topological relations computation between volumes. *Sci. Surv. Map.*, 37(4), 120-122. doi.org/10.16251/j.cnki.1009-2307.2012.04.052
- Shen, J.W., Zhou, T.G., Zhu, X.B., 2016. A topological relation description model for areal objects with holes. *Acta Geod. Cartogr. Sin.*, 45(6), 722-730.
- Shu, Q.G., Wu, Q.L., Luo, G., Liu, H., He, L.H., Zheng, M.X., 2024. Evolution of morphological characteristics of Qingju central bar under curved river hydropower development. *J. China West Norm. Univ. Nat. Sci. Ed.*, 45(6), 632-638. doi.org/10.16246/j.issn.1673-5072.2024.06.009
- Wang, L.X., Dai, Z.J., Mei, X.F., Wang, J., Lou, Y.Y., Qiao, H.J., 2024. Dynamic geomorphic change process of central bars at the bifurcation of North and South Branches in Yangtze Estuary. *Mar. Sci. Bull.*, 43(5), 595-607.
- Zhang, J., Qi, X.L., 2008. Topological analysis between bodies with holes. *Int. J. Comput. Sci. Netw. Secur.*, 8(8), 167-174.